

PREPARATION OF HIGH-TOUGHNESS THERMOPLASTIC STARCH FILMS VIA ENZYMATIC HYDROLYSIS AND CROSS-LINKING MODIFICATION

Hao Wang, ChuanWei Zhang*

College of Mechanical and Electrical Engineering, Qingdao University, Qingdao 266071, Shandong, China.

Corresponding Author: ChuanWei Zhang, Email: zhangchuanwei3722@163.com

Abstract: Unlike traditional petroleum-based thermoplastic films, starch-based films rely on solvent systems and cannot be processed thermally, resulting in low production efficiency and hindering large-scale industrial applications. This study developed a dual-modification method combining enzymatic hydrolysis, dual cross-linking, and plasticizers to prepare enzyme-crosslinked thermoplastic starch (ECSS). High-toughness and transparent films were fabricated via hot-pressing technology. Enzymatic hydrolysis reduced starch crystallinity and molecular chain entanglement, facilitating subsequent cross-linking reactions. Citric acid (CA) and sodium trimetaphosphate (STMP) synergistically constructed a dense molecular cross-linked network through esterification and phosphorylation, respectively. With the assistance of plasticizers, the tensile strength of the film increased by 62.3%, and the elongation at break reached 348.7%. Thermogravimetric analysis (TGA) confirmed that dual cross-linking significantly enhanced thermal stability. Differential scanning calorimetry (DSC) revealed a reduced glass transition temperature (T_g), indicating improved thermoplasticity. X-ray diffraction (XRD) demonstrated that cross-linking effectively disrupted the crystalline structure of starch, forming a stable amorphous network.

Keywords: Thermoplastic starch; Enzymatic hydrolysis; Cross-linking; High-toughness film

1 INTRODUCTION

Petroleum-derived materials are widely used in industries such as plastics, synthetic fibers, and coatings due to their cost-effectiveness and superior performance [1]. However, their environmental impacts, including pollution due to non-biodegradability, resource depletion, and carbon emissions, are undeniable [2]. The finite nature of petroleum resources, coupled with their ecological drawbacks, has spurred the search for sustainable alternatives. In recent years, significant efforts have been directed towards the development of biodegradable materials. Starch, a renewable natural polysaccharide derived from various crops, has emerged as one of the most promising feedstocks for biodegradable plastics [3]. Unlike petroleum-based polymers, starch molecules contain abundant hydroxyl groups that form strong intermolecular hydrogen bonds [4], resulting in a melting temperature that exceeds the thermal decomposition threshold. This inherent property renders native starch non-thermoplastic and unsuitable for melt processing [5].

To enhance the processability of starch-based materials, enzymatic modification using α -amylase has been explored to reduce molecular weight and crystallinity, thereby enabling thermoplastic behavior [6,7]. While enzymatically hydrolyzed starch exhibits improved adsorption capacity and delayed degradation, it suffers from inferior shear resistance compared to native starch [8]. To address this limitation, dual modification strategies combining enzymatic and chemical treatments have been proposed. For instance, Karim et al. [9] employed a hybrid approach involving fungal α -amylase/glucosylase-mediated hydrolysis followed by hydroxypropylation with propylene oxide. The modified starch demonstrated enhanced functionality compared to unmodified counterparts. These findings underscore the potential of dual modification to overcome the mechanical deficiencies of enzymatically treated starch [10].

Chemical modifications, including oxidation, esterification, ionization, grafting, and cross-linking, are commonly employed to tailor starch properties for diverse applications [11]. Among these, cross-linking is the most prevalent technique, aimed at replacing hydrogen bonds in crystalline regions with covalent bonds (e.g., ether, phosphodiester, or organic ester linkages) to stabilize molecular networks [12]. Enzymatic hydrolysis disrupts starch chains, reducing molecular weight and disentangling helical structures [13], while subsequent cross-linking reconnects adjacent chains via ester/ether bonds [14], thereby enhancing structural integrity and restricting chain mobility. Conventional cross-linkers such as epichlorohydrin (EPI) [15], glucose-malonaldehyde [16], glutaraldehyde [17], and polyurethanes [18] face challenges including high cost, toxicity, or inefficiency. In contrast, citric acid (CA) and sodium trimetaphosphate (STMP) [19, 20] offer eco-friendly alternatives. CA enables esterification with starch hydroxyl groups under sub-gelatinization [21, 22] or heat-moisture conditions [23], forming multi-chain cross-linked networks. STMP introduces phosphate ester bonds, improving mechanical strength, thermal resistance, and water stability [24]. Their non-toxic nature, high efficiency, and compatibility with enzymatic pretreatment make CA/STMP ideal for green manufacturing of thermoplastic starch with enhanced toughness and tensile strength [25].

Cross-linking efficiency and starch properties are highly dependent on reaction parameters such as temperature, duration, pH, additive concentration, and moisture content [26]. While dry/semi-dry methods achieve satisfactory cross-linking, their high energy demands (120–160 °C) limit scalability [27]. Wet cross-linking at 40–70 °C offers a low-energy, facile alternative with precise process control. Additives further optimize reactions by activating starch

binding sites. For example, Xie et al. [28] utilized Na_2SO_4 to suppress hydrolysis and stabilize active sites, albeit generating saline wastewater. Environmentally benign additives like urea and glycerol are preferred: urea enhances plasticity through hydrophobic interactions[29], while glycerol prevents chain hardening during cross-linking [30]. Their synergistic effects improve reaction efficiency, flexibility, and thermal stability. This study aims to resolve the trade-off between thermoplastic processability and mechanical robustness in starch films. We developed a dual-modified starch (ECSS) via α -amylase-assisted hydrolysis followed by CA/STMP cross-linking, with urea/glycerol as plasticizers. Comparative analyses of native starch (NS), enzymatically hydrolyzed starch (ES), and single-crosslinked starches (ECS: CA; ESS: STMP) were conducted to elucidate the superiority of dual cross-linking. The films were characterized through macroscopic observation, mechanical testing (tensile strength, elongation), thermal analysis (DSC, TGA), melt flow rate (MFR), and microstructural techniques (FTIR, XRD, SEM). These investigations provide mechanistic insights into the fabrication of high-toughness, transparent starch-based films.

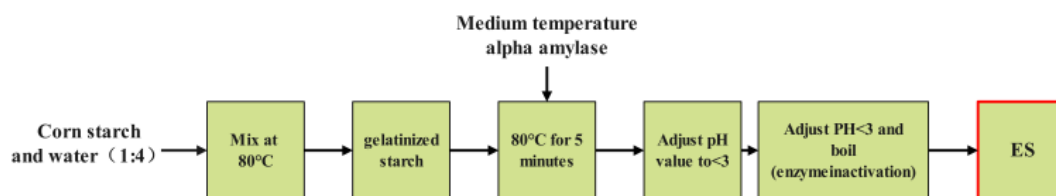


Figure 1 Process Diagram of Enzymatic Hydrolysis of Starch

2 EXPERIMENTAL MATERIALS AND METHODS

2.1 Experimental Materials

The starch used in this study was ordinary corn starch. Other chemicals and reagents included medium-temperature α -amylase (2U/mg), hydrochloric acid, sodium hydroxide, urea, citric acid, sodium tripolyphosphate, and montmorillonite, all purchased from Macklin Company (Shanghai, China). Glycerol was obtained from Shanghai Hushi.

2.2 Preparation of ES, ECS, ESS, and ECSS

The general preparation process for ES, ECS, ESS, and ECSS is outlined in Figure 1. The preparation method for ES is as follows: 20 g of corn starch was added to 80 mL of deionized water in a round-bottom flask and stirred rapidly in a water bath at 80 °C until the starch was completely gelatinized. Then, 0.05 g of medium-temperature α -amylase was dissolved in 10 mL of water and added to the gelatinized starch. The mixture was stirred for an additional 5 minutes to obtain a liquefied starch solution. This solution was then rapidly cooled in ice water to halt the enzymatic reaction. To adjust the pH of the solution below 3, 1 mol/L hydrochloric acid was added dropwise. The mixture was heated in a boiling water bath for 5 minutes and then cooled again in ice water. Once the solution reached room temperature, 1 mol/L sodium hydroxide was added to neutralize the hydrochloric acid, deactivating the enzyme. The enzymatic solution was then poured into a Teflon dish and dried in a vacuum oven at 70 °C for 24 hours to obtain ES.

For ECS, 30 g of enzymatically modified starch was mixed with 100 mL of deionized water in a round-bottom flask, and 9 g of citric acid was added. The mixture was stirred for 5 minutes. Sodium hydroxide (1 mol/L) was added dropwise to adjust the pH to 5.5. Next, 2 g of citric acid and 1 g of glycerol were added, and the mixture was stirred at 70 °C for 2 hours. After washing and drying, the product was placed in a Teflon dish with a PTFE sheet and dried in a vacuum oven at 40 °C for 48 hours to obtain ECS.

For ESS, 30 g of enzymatically modified starch was mixed with 100 mL of deionized water in a round-bottom flask, and sodium hydroxide (1 mol/L) was added to adjust the pH to 10. Then, 2 g of urea and 1 g of glycerol were added, followed by 9 g of sodium tripolyphosphate. The mixture was stirred in a water bath at 40 °C for 2 hours. After washing and drying, the product was placed in a Teflon dish with a PTFE sheet and dried in a vacuum oven at 40 °C for 48 hours to obtain ESS.

To prepare ECSS, the methods for ECS and ESS were combined. 30 g of enzymatically modified starch was mixed with 100 mL of deionized water, and 9 g of citric acid was added and stirred for 5 minutes. Sodium hydroxide (1 mol/L) was added to adjust the pH to 5.5, followed by 2 g of citric acid and 1 g of glycerol. The mixture was stirred at 70 °C for 2 hours. Sodium hydroxide (1 mol/L) was then added to adjust the pH to 10, and 9 g of sodium tripolyphosphate was added. The mixture was stirred in a water bath at 40 °C for 2 hours. After washing and drying, the product was placed in a Teflon dish with a PTFE sheet and dried in a vacuum oven at 40 °C for 48 hours to obtain ECSS.

2.3 Preparation of Modified Films

The modified starch prepared in Section 2.2 was used to produce films. An appropriate amount of dried starch was selected and compressed using a hot press at 0.5 MPa pressure and 40 °C for 2 minutes. After cooling for 5 minutes, starch-based films were obtained.

2.4 Optical Observation and Scanning Electron Microscopy

The prepared films were visually examined under bright light to assess their appearance, light transmittance, and transparency. The films were gold-coated and observed using a scanning electron microscope (JEOL-JSM6400, Tokyo, Japan) to examine their internal structure.

2.5 Microstructural Characterization of Modified Starch Molecules

2.5.1 FTIR Analysis

Fourier transform infrared spectroscopy (FTIR; Nicolet iS20, Thermo Fisher Scientific, USA) was employed to analyze the chemical structure of the modified starch films. FTIR spectra were recorded in the range of 400 to 4000 cm^{-1} for each sample.

2.5.2 XRD

X-ray diffraction (XRD; MiniFlex 600, Rigaku, Japan) was used to analyze the powders of NS and other samples. The samples were prepared with uniform thickness, and their surfaces were aligned parallel to the glass frame. The scan was conducted at a speed of 2°/min for angles ranging from 10° to 60°. Before testing, the samples were dried at 50 °C for 12 hours to prepare an anhydrous sample.

2.6 Mechanical Performance Testing

Mechanical testing was performed using a universal testing machine (Instron 3367, Illinois Tool Works Inc.) to measure the tensile strength and elongation at break of the hot-pressed films. Each sample, cut to a length of 35 mm and a thickness of 1 mm, underwent five tests at room temperature, and the average value was recorded.

2.7 Thermal Performance Analysis

2.7.1 Thermogravimetric Analysis (TGA)

Thermogravimetric analysis (TGA) was conducted using a TASDT650 synchronous thermal analyzer to assess the thermal stability of the films. Samples weighing approximately 5 mg were heated from room temperature to 450 °C at a heating rate of 10 °C/min.

2.7.2 Differential Scanning Calorimetry (DSC)

Differential scanning calorimetry (DSC) was used to evaluate the thermal stability of the materials. Each sample was heated from room temperature to 150 °C at a rate of 10 °C/min.

2.7.3 Melt Flow Rate (MFR)

The Melt Flow Rate (MFR) of the samples was tested according to the standard GB/T 3682.1-2018 D method. The tests were conducted at different temperatures and loading conditions to analyse the thermoplasticity and processing adaptability of the materials.

Two standard loading conditions were set for this experiment:

Standard test force No. 2: 1.2 kg, corresponding to approximately 11.77 N (formed by a base load of 0.325 kg plus a counterweight of 0.875 kg);

Standard test force No. 3: 2.16 kg, corresponding to approximately 21.18 N (base load 0.325 kg plus 1.835 kg counterweight).

The test temperatures were set at 120 °C and 150 °C, which, in combination with the two pressure conditions, constituted four sets of experimental conditions. The samples were heated to soften under the set conditions and then extruded through a die of specified diameter. During the extrusion process, the melt strip was truncated every 20 seconds. For each set of conditions, five homogeneously truncated melt sample strips were selected and weighed, and their average mass was calculated. The resulting data were entered into a calculating device that automatically converted the melt flow rate (in g/10min). The test was repeated five times for each sample and the average value was taken to ensure the stability and representativeness of the experimental data.

2.8 Water Contact Angle Testing

The films were placed horizontally on the experimental platform, and 50 μL of distilled water was added each time. Once the value stabilized, the water contact angle was recorded using software. Each sample was tested five times, and the average value of the five measurements was calculated.

2.9 Water Vapour Transmission (WVT)

The water vapour transmission rate of the samples is measured using a modified version of the 'cup method' of ASTM E96-95. The test was carried out at constant temperature and humidity to evaluate the water vapour barrier properties of the films.

Firstly, the prepared starch-based films were cut into standard circles with a diameter of 65 mm and laid flat on a test cup previously filled with distilled water, making sure that the edges were sealed tightly to prevent lateral permeation. The test device was then pre-treated in a constant temperature and humidity environment with a relative humidity of

50% and a temperature of 23 ± 2 °C until the samples reached a constant state of mass, ensuring that water vapour transport occurred predominantly in the vertical direction of the film.

During the experiment, the mass change of the cup assembly was recorded every 30 minutes, and the water vapour transmission rate was calculated by monitoring the mass loss due to water evaporation. The WVT value was calculated using the following formula:

$$\text{WVT} = \frac{\Delta_m}{\Delta_t \cdot S} \quad (1)$$

Δ_m Weight loss for water, Δ_t is the experimental time, S is the film area.

3 RESULTS AND DISCUSSION

3.1 Film Morphological Analysis

Figure 2 presents both macroscopic images and cross-sectional scanning electron microscope (SEM) images of the films, which were prepared from various modified starches using hot pressing. These images are used to characterize the morphology of the films. The ECS film shows moderate transparency and a rough texture, with numerous voids and bubbles, as depicted in Figure 2a. The ESS film appears opaque, featuring a smooth surface with some internal bubbles and cracks, as shown in Figure 2b. In contrast, the ECSS film has a smooth surface, free from cracks or bubbles, and demonstrates excellent transparency, as shown in Figure 2c. These results suggest that the ECSS-modified starch films exhibit favorable morphology, confirming that the preparation method is viable.

Following enzymatic hydrolysis, the issue of molecular chain entanglement was resolved, allowing for improved thermal processing. Figures 2d, e, and f display the internal structures observed under SEM. After hot pressing, the films show no distinct starch granules, and the integrity of the starch granules is reduced. This indicates that the films possess thermoplastic properties. Compared to Figures 2d and e, Figure 2f shows a more uniform internal structure, suggesting that the ECSS film has superior thermoplastic properties.

From the SEM images, clear differences in the internal structure and bonding states of the starch films can be observed. Figure 2g (ECS film) displays surface layering and cracking, which suggests a relatively loose network structure and insufficient uniformity. Figure 2h (ESS film) shows a loose internal structure with more cracks, likely due to the high crosslinking density resulting from the crosslinking process, but without adequate flexible regulation. In contrast, Figure 2i (ECSS film) exhibits a smooth and uniform surface with no visible cracks or pores, and the internal structure is dense and consistent. This observation fully demonstrates the synergistic effect of citric acid and sodium tripolyphosphate double crosslinking, as well as the enhancement of material flexibility and uniformity through the use of plasticizers. These findings indicate that ECSS significantly outperforms the other two materials in terms of internal structure and bonding state.

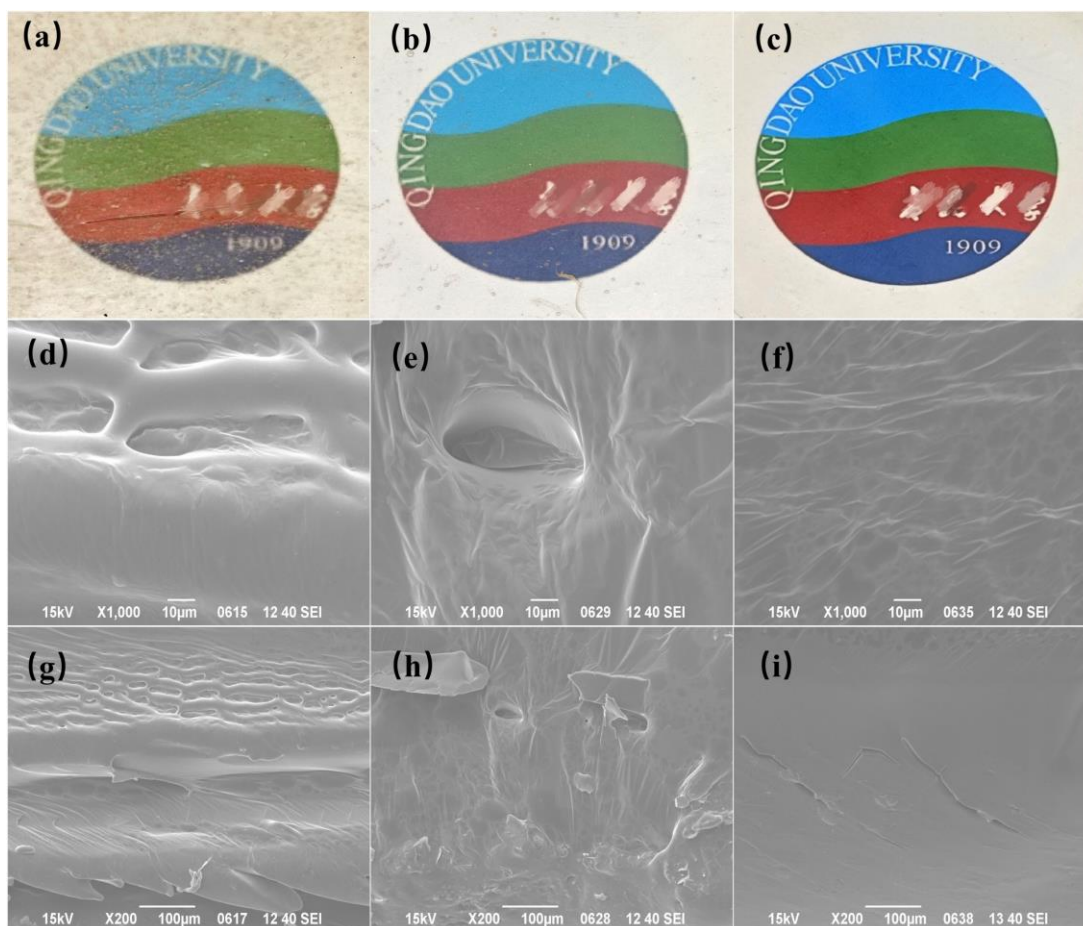


Figure 2 (a, b, c) Macroscopic Images Showing Starch Films after Hot Pressing with the Internal Structure of Different Starch Films under Electron Microscopy. (a, d, g) ECS, (b, e, h) ESS, (c, f, i) ECSS

3.2 Molecular Change Analysis

3.2.1 FTIR analysis

The Fourier transform infrared (FTIR) absorption spectra of native starch (NS), enzymatically hydrolyzed starch (ES), citric acid-crosslinked starch (ECS), sodium tripolyphosphate-crosslinked starch (ESS), and double-crosslinked starch (ECSS) are shown in Figure 3. In the FTIR spectra, NS exhibits a broad peak at 3314 cm^{-1} , corresponding to the O-H stretching vibration, which indicates the abundance of hydroxyl groups in the starch molecules. After enzymatic hydrolysis and crosslinking modifications, the O-H stretching vibration peaks of the modified samples (ES, ECS, ESS, ECSS) gradually shift to lower wavenumbers (e.g., ECSS at 3267 cm^{-1}). This shift suggests that crosslinking and plasticizing reactions enhance intermolecular hydrogen bonding while reducing the number of free hydroxyl groups. This implies that the introduction of citric acid, sodium tripolyphosphate, and plasticizers (such as glycerol and urea) significantly alters the intermolecular interactions in starch.

In the $1550\text{-}1700\text{ cm}^{-1}$ region, a new C=O stretching vibration peak appears in ECS, which is a characteristic feature of ester bond formation between citric acid and the hydroxyl groups of starch molecules, confirming the crosslinking effect of citric acid. In ESS, enhanced peaks in the $900\text{-}1200\text{ cm}^{-1}$ region (particularly around 1150 cm^{-1} and 1040 cm^{-1}) correspond to the vibrations of P=O and P-O-C bonds, indicating the presence of phosphoester crosslinking introduced by sodium tripolyphosphate. Additionally, the reduced intensity of the O-H peak in ESS suggests that some hydroxyl groups are involved in forming phosphoester bonds.

The FTIR spectrum of the double-crosslinked sample (ECSS) shows a combination of features from both the single-crosslinked materials. The C=O esterification vibration peak in the $1550\text{-}1700\text{ cm}^{-1}$ region and the phosphoester characteristic peak in the $900\text{-}1200\text{ cm}^{-1}$ region are both significantly enhanced, indicating that citric acid and sodium tripolyphosphate collaboratively participate in the crosslinking reaction, forming a denser intermolecular crosslinked network. Furthermore, the O-H vibration peak in ECSS shifts further to 3267 cm^{-1} compared to the other samples, suggesting that the double-crosslinking system significantly strengthens the intermolecular hydrogen bonding, thereby enhancing the structural stability of the starch material.

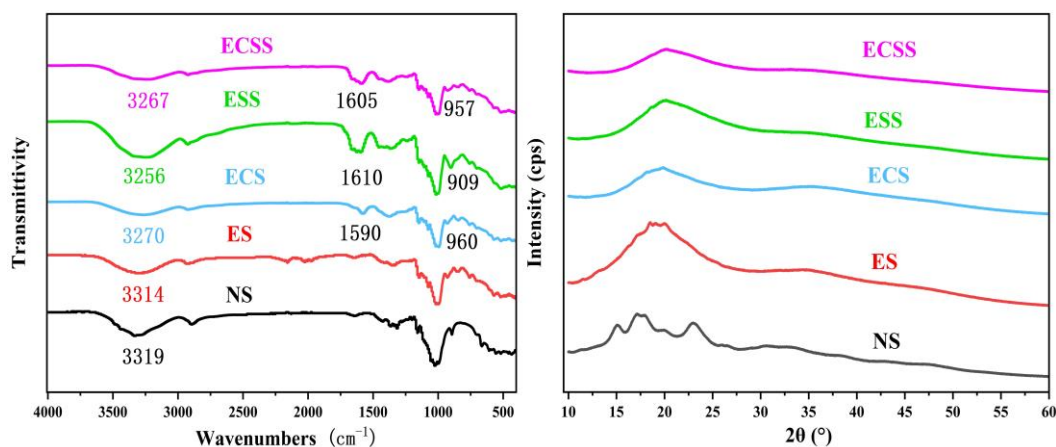


Figure 3 FTIR Absorption Spectra and XRD Spectra of NS, ES, ECS, ESS

3.2.2 XRD analysis

The X-ray diffraction (XRD) spectra reveal significant changes in the crystal structure of the starch samples during the modification process. Native starch (NS) shows typical A-type crystal diffraction peaks at 15°, 17°, 20°, and 23°, indicating a high degree of crystallinity. However, after enzymatic hydrolysis (ES), these characteristic diffraction peaks are noticeably weakened, indicating that the enzymatic treatment disrupted part of the ordered crystalline structure in the starch molecules. Further crosslinking modifications (ECS and ESS) cause the diffraction peaks to weaken and broaden, suggesting that the crosslinking effects of citric acid and sodium tripolyphosphate significantly disrupt the molecular chain order, rendering the material more amorphous. Notably, for the double-crosslinked sample (ECSS), the diffraction peaks almost disappear, indicating a highly amorphous structure. This suggests that the double-crosslinking reaction not only disrupts the crystalline regions but also creates a denser amorphous network.

This trend of decreasing crystallinity is consistent with the changes observed in the FTIR spectra. For instance, the -OH stretching vibration peaks (3256 cm⁻¹ and 3267 cm⁻¹) in ECS and ESS are significantly reduced, suggesting that the crosslinking reaction consumes hydroxyl groups, thereby decreasing the hydrogen bonding between molecular chains. This change in chemical bonds further disrupts the ordered structure of the crystalline regions, leading to the weakening of the diffraction peaks in the XRD analysis. Therefore, by combining the XRD and FTIR analyses, it is evident that the synergistic effects of enzymatic hydrolysis and crosslinking modifications drive the starch material's transition from a crystalline to an amorphous state. This transition 'imparts enhanced mechanical properties and processability to the starch-based films.

3.3 Thermal Performance Analysis

3.3.1 Thermogravimetric Analysis (TGA)

The thermogravimetric analysis (TGA) spectra highlight significant variations in the thermal decomposition behaviors of the starch samples treated under different conditions. Native starch (NS) exhibits the lowest onset temperature for thermal decomposition, approximately 250 °C. This can be attributed to its molecular structure, where hydrogen bonding predominates and there is an absence of chemical crosslinking, which contributes to its relatively poor thermal stability. The enzymatically modified starch (ES) shows a slight increase in the onset temperature of decomposition, around 260 °C. This improvement is likely due to the partial breaking of molecular chains during enzymatic hydrolysis, which reduces the crystalline regions and moderately enhances thermal degradation properties. However, the overall thermal stability is still limited since no substantial crosslinking network is formed within the structure.

In contrast, the citric acid-crosslinked starch (ECS) demonstrates a notable increase in the thermal decomposition onset temperature, reaching above 270 °C. This indicates that citric acid induces the formation of stable chemical crosslinking bonds through esterification, thereby enhancing the structural integrity and thermal stability of the starch. The sodium tripolyphosphate-crosslinked starch (ESS) further elevates the decomposition onset temperature to around 300 °C. This enhancement is attributed to the formation of phosphoester bonds, which increase the crosslinking density between the molecules, thus further improving thermal stability. The double-crosslinked sample (ECSS) exhibits the highest thermal decomposition onset temperature, exceeding 300 °C. This suggests that the synergistic effect of citric acid and sodium tripolyphosphate, through the formation of a dense double-crosslinked network, significantly boosts molecular stability and resistance to thermal degradation.

As shown in Figure 4, the weight loss curves during thermal decomposition reveal that NS and ES undergo rapid, single-stage decomposition, exhibiting relatively straightforward degradation behavior. Conversely, the weight loss curves for ECS, ESS, and ECSS show multi-stage decomposition, indicating that crosslinking modifications have enhanced the complexity of the molecular chains, thereby delaying the onset of primary decomposition. Additionally, the ECSS sample retains the highest residual char content at elevated temperatures (>350 °C), further confirming that the double-crosslinked structure improves both thermal stability and the material's ability to undergo carbonization.

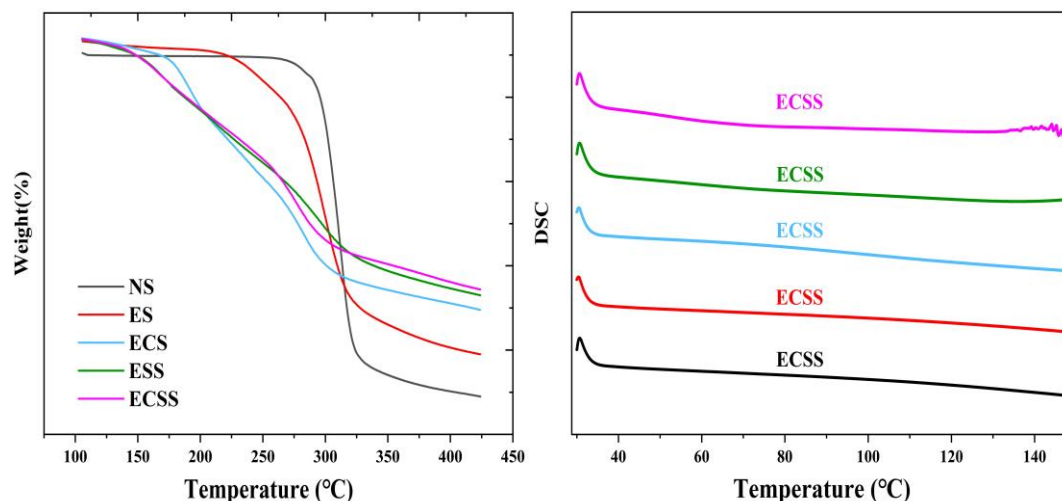


Figure 4 TGA (a) and DSC (b) Mapping of NS, ES, ECS, ECS, ECSS

3.3.2 Thermal Melt Performance (DSC)

The differential scanning calorimetry (DSC) spectra reveal distinct differences in the thermal properties of the starch samples in the temperature range of 40 °C to 150 °C. These variations primarily reflect the relationship between molecular chain arrangements, the formation of the crosslinked network, and the resulting thermal stability. The ECSS sample demonstrates the most gradual heat flow curve, suggesting significantly superior thermal stability compared to the other samples. This improvement in thermal stability is primarily attributed to the formation of the double-crosslinked network. Citric acid and sodium tripolyphosphate, by forming ester and phosphoester bonds, respectively, work synergistically to increase the crosslinking density between starch molecules. The crosslinked network not only limits the thermal motion of the molecular chains but also enhances overall thermal stability. Moreover, the addition of glycerol and urea as plasticizers optimizes the flexibility and distribution of the molecular chains, resulting in better heat resistance.

In contrast, the DSC curves of the ECS and ESS samples demonstrate relatively lower thermal stability, slightly inferior to that of the ECSS sample. Although single crosslinking modifications can increase bonding strength and crosslinking density, the limited number of crosslinking sites results in a weaker network structure and lower stability. Among these, the ESS sample shows better thermal stability in the medium-to-high temperature range compared to ECS, likely due to the more stable chemical structure provided by the phosphoester bonds formed by sodium tripolyphosphate in specific temperature ranges. The ES sample, however, exhibits a more pronounced decline in the heat flow curve, indicating poor thermal stability. The absence of chemical crosslinking support between the molecular chains—relying only on physical interactions—leads to easier decomposition when heated. Furthermore, the DSC curve of NS shows the most significant decrease in heat flow, indicating that the unmodified starch structure is more loosely organized, with weak intermolecular cohesion, making it highly susceptible to thermal degradation.

3.3.3 MFR

Melt flow rates of different samples under DIFFERENT TEMPERATURE and pressure conditions can be seen in table 1 and the melt flow rates of NS, ES, TPS, and ETPS measured under standard test forces at different temperatures and adaptability levels (120 ° C and 150 ° C) with adapta can be seen in figure 5.

Table 1 Melt Flow Rates of Different Samples under DIFFERENT TEMPERATURE and Pressure Conditions

Materials	Solute flow rate (g/10 min)			
	120°C和 11.77N	120°C and 21.18 N	150°C and 11.77 N	150°C and 21.18N
NS	0	0	0	0
ES	0	0	0	0
ECS	0.88 (±0.21)	5.09 (±0.34)	1.38 (±0.16)	5.74 (±0.49)
ESS	1.43 (±0.23)	8.27 (±0.49)	2.24 (±0.35)	9.33 (±0.76)
ECSS	1.87 (±0.35)	10.81 (±0.87)	2.93 (±0.31)	12.2 (±0.88)

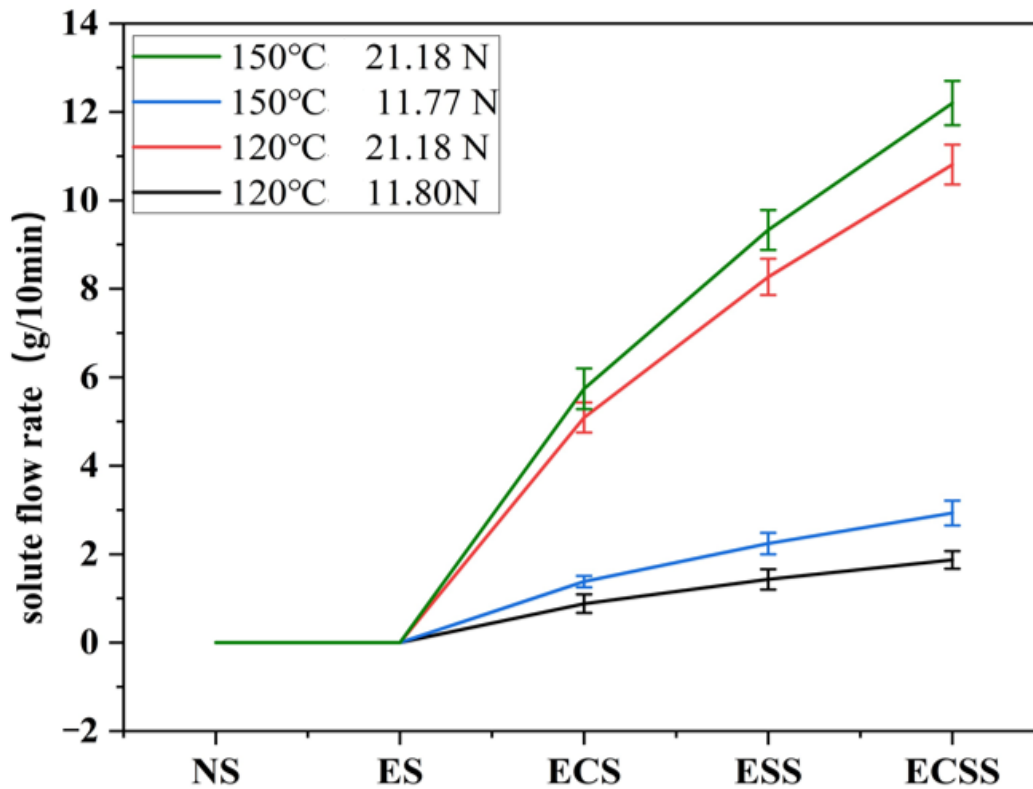


Figure 5 The Melt Flow Rates of NS, ES, TPS, and ETPS Measured under Standard Test Forces at Different Temperatures and Adaptability Levels (120 °C and 150 °C) with Adapta

3.4 Starch Film Mechanism Analysis

As illustrated in Figure 6, the crosslinking reaction between sodium tripolyphosphate (STMP) and citric acid influences the starch structure through distinct mechanisms. Sodium tripolyphosphate reacts with the hydroxyl groups in the starch molecules, forming phosphoester bonds. These bonds create a dense network structure that enhances the overall stability of the film. In contrast, citric acid undergoes esterification, where its carboxyl group forms ester bonds with the hydroxyl groups in the starch. This further strengthens the crosslinking effect while imparting some flexibility to the material.

Glycerol and urea serve as plasticizers, providing additional support. Glycerol, with its multi-hydroxyl structure, forms hydrogen bonds with the starch molecular chains, while urea, through its amino and carbonyl groups, interacts with the hydroxyl groups in starch. This interaction not only prevents excessive hardening of the chains during the crosslinking process but also enhances the flexibility and toughness of the material. Furthermore, this combination improves the overall flowability and ductility of the starch-based films.

In conclusion, the synergistic effects of these components result in starch films that demonstrate both flexibility and strength. This combination of properties makes the films more adaptable and resilient, thereby improving their suitability for various applications.

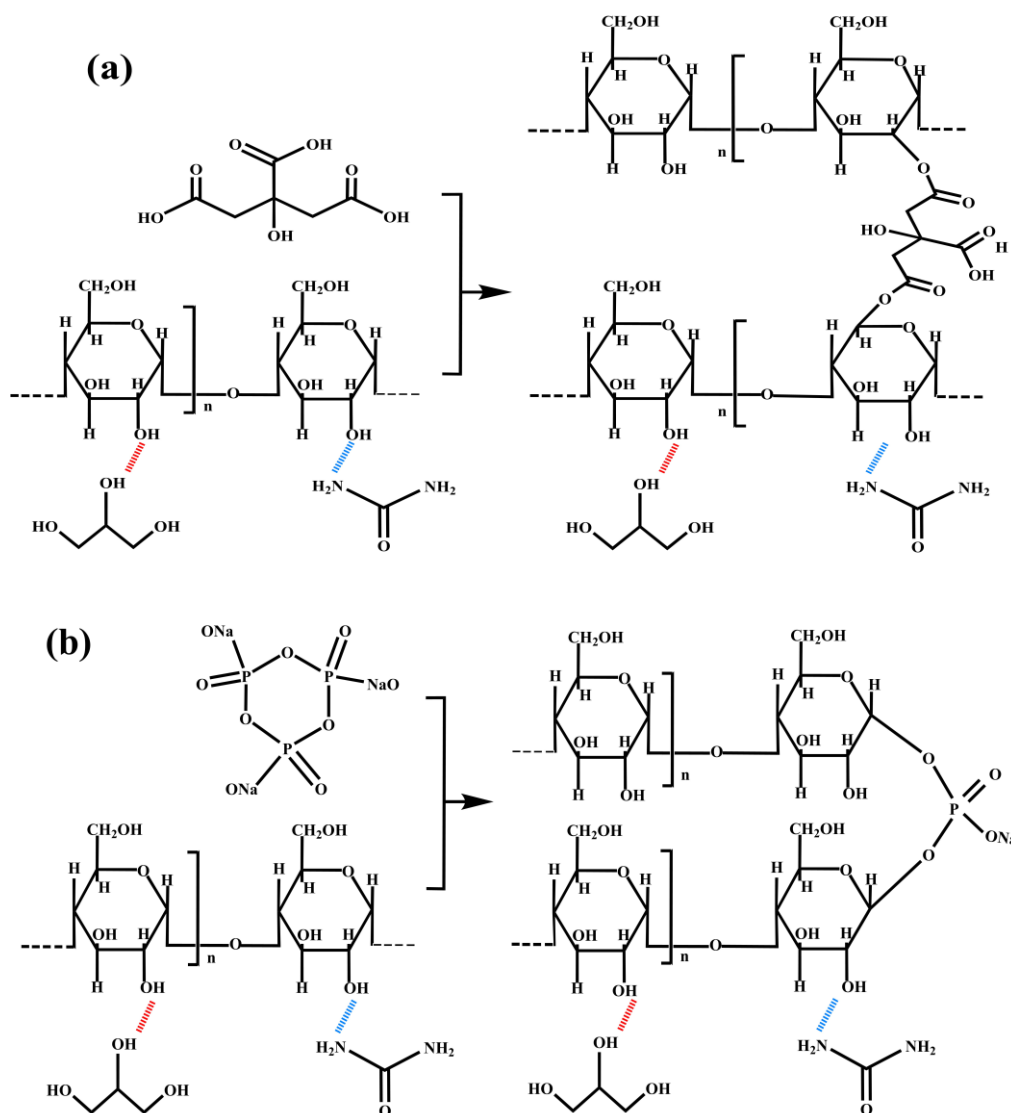


Figure 6 Crosslinking Mechanism Diagram, (a) Citric acid Crosslinking Mechanism Diagram, (b) Sodium Tripolyphosphate Crosslinking Mechanism Diagram

3.5 Mechanical Performance Analysis

As shown in the mechanical performance chart (Figure 7), the ECSS film demonstrates significantly superior tensile strength and elongation at break compared to the other samples. The tensile strength of ECSS is 1.61 MPa, substantially higher than that of the single-crosslinked ESS (1.02 MPa), ECS (0.63 MPa), and the unmodified enzymatically hydrolyzed starch ES (0.12 MPa). This considerable improvement is attributed to the formation of a double-crosslinked network, where the esterification reaction of citric acid and the phosphoester bonds formed by sodium tripolyphosphate work synergistically to increase the crosslinking density between molecules, leading to a substantial enhancement in the material's strength.

Despite its high tensile strength, the ECSS film also exhibits a remarkable elongation at break of 351.45%, which is significantly higher than the values observed for ESS (175.39%) and ECS (210.64%). This phenomenon suggests that the synergistic effect of the double-crosslinking not only increases the rigidity of the molecular chains but also enhances their flexibility. The plasticizers, glycerol and urea, form hydrogen bonds with the starch molecular chains, reducing intermolecular cohesion and increasing the flexibility of the chains. Additionally, the increased proportion of amorphous regions further facilitates the mobility of the molecular chains, which in turn improves the elongation at break.

The X-ray diffraction (XRD) spectra of the ECSS sample reveal the weakest diffraction peaks, indicating that the double-crosslinking reaction significantly disrupts the crystalline structure of the starch, resulting in a material that is almost entirely amorphous. This observation aligns with the high elongation at break seen in the mechanical performance, as the amorphous structure enhances the material's toughness, making it more ductile during stretching.

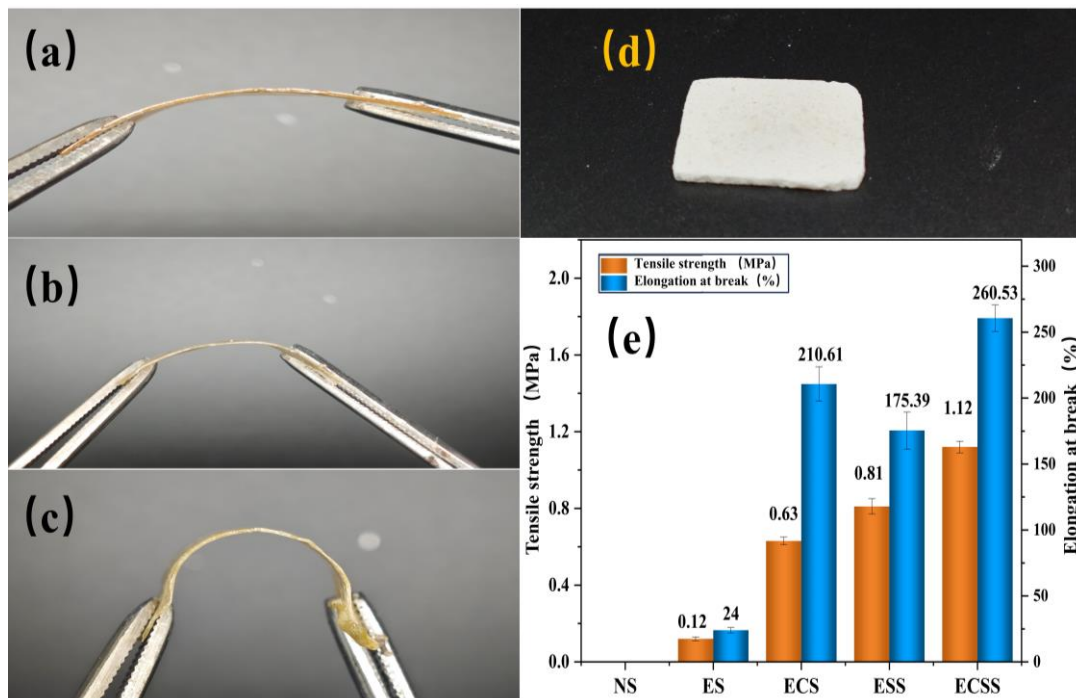


Figure 7 Comparison of Mechanical Properties of Hot Pressed Specimens with Different Modified Specimens, (a) ECS Hot Pressed Specimens (b) ESS Hot Pressing Specimen (c) ECSS Hot Pressing Specimen, (d) Comparison of Tensile Strength and Elongation at Break of Different Specimens

3.6 Water Contact Angle Analysis

The water contact angles of different film samples are shown in Figure 8. Starch is inherently hydrophilic; however, its water resistance can be significantly enhanced through modification. The results of the water contact angle tests, presented in the figure, reveal notable differences in water resistance among the ECS, ESS, and ECSS films. The water contact angle for the ECS film is 33.14° , indicating that the citric acid-crosslinked film retains some hydrophilic properties. This is attributed to the polar groups introduced by the carboxyl and ester bonds formed during the esterification reaction of citric acid, which increases the film's ability to absorb water molecules.

The water contact angle for the ESS film is 29.06° , which is lower than that of ECS. This reduction is likely due to the higher hydrophilicity of the phosphoester bonds formed by the sodium tripolyphosphate crosslinking, resulting in increased water absorption on the film surface. In contrast, the water contact angle for the ECSS film increases substantially to 51.02° , demonstrating its superior water resistance compared to the single-crosslinked films. This enhanced performance is attributed to the double-crosslinking effect of citric acid and sodium tripolyphosphate, which creates a denser crosslinked network between molecules, thereby reducing the surface free energy of the material. Additionally, the incorporation of plasticizers reduces the exposure of polar groups within the film.

In conclusion, the double-crosslinking system significantly improves the water resistance of starch-based films, offering reliable support for enhancing their water-resistant performance in practical applications.

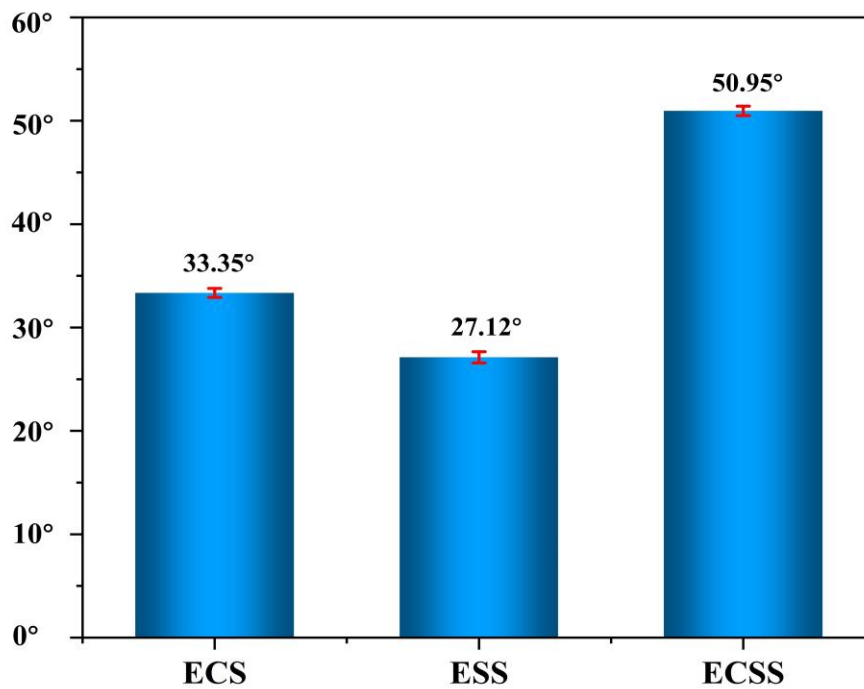


Figure 8 Water contact Angle of Different Film Samples: (a) ECS Film、(b) ESS、Film、(c) ECSS Film

3.7 Water Vapour Transmission (WVT)

The water vapour transmission rate values of the different samples are shown in Figure 9. As shown in the figure, the water vapour transmission rate values of all the three samples are high and the water repellency is not considered to be excellent. The water vapour transmission rate of the ECS film is the highest among the three samples at 14.5×100 ($\text{g}^2/\text{m} \times 24\text{h}$), which is due to the fact that the single citric acid cross-linking (ECS), although it improves the densification of the film to a certain extent, fails to inhibit the water vapour permeation effectively due to the high number of flexible chain segments. The WVT value of the sample ESS film was reduced by 13.8×100 ($\text{g}^2/\text{m} \times 24\text{h}$) to whereas the introduction of sodium trimetaphosphate for crosslinking (ESS) led to the formation of phosphate bonds in the system and the network structure was further strengthened, which made the water molecule penetration pathway more complex, thus reducing the WVTR value. The WVT value of the ECSS film is 12.9×100 ($\text{g}^2/\text{m} \times 24\text{h}$), which is the lowest among the three films. This is because the double cross-linking leads to the construction of a denser three-dimensional cross-linking network structure between the molecules, which effectively fills up the free volume between the polymer chains, and enhances the shielding effect of the film against water vapour.

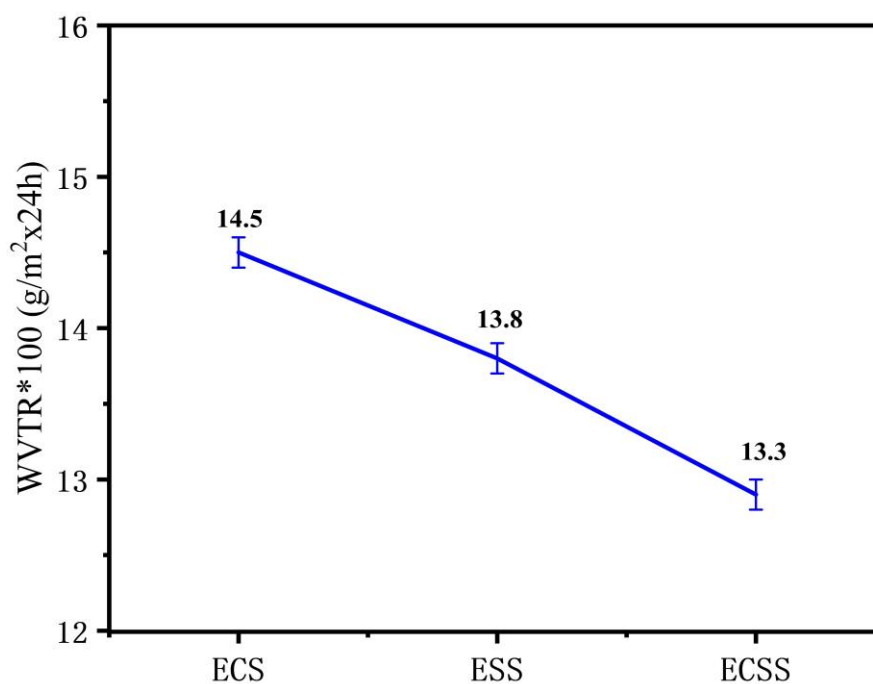


Figure 9 Water Vapor Permeability of Different Samples

4 CONCLUSIONS

This study successfully developed a double-crosslinked modified starch (ECSS) with enhanced thermoplastic properties by employing a synergistic modification strategy involving enzymatic hydrolysis, citric acid esterification, and sodium tripolyphosphate crosslinking. The resulting films demonstrated high toughness and transparency. The structural changes and performance enhancement mechanisms during the modification process were systematically investigated. Enzymatic hydrolysis significantly reduced the length and crystallinity of the starch molecular chains, minimized chain entanglement, and greatly improved the mobility of the molecular chains, thus providing a foundation for subsequent chemical modifications.

The esterification of citric acid and phosphoesterification of sodium tripolyphosphate formed a stable, three-dimensional crosslinked network between starch molecules, imparting the material with superior mechanical properties, thermal stability, and water resistance. Additionally, the incorporation of glycerol and urea as plasticizers enhanced the starch's flexibility and toughness, while effectively preventing the closure of hydroxyl active sites and improving the uniformity and efficiency of the crosslinking reaction.

After thermal processing, the modified starch films exhibited excellent thermal stability and mechanical strength. The results confirmed that the double-crosslinking modification significantly improved the material's thermal stability and mechanical strength, enabling the films to retain better shape stability at high temperatures. Mechanical performance testing revealed outstanding flexibility and tensile properties.

The enzymatic double-crosslinking modification strategy proposed in this study offers a novel solution to overcome the limitations of starch-based materials in thermoplastic processing. Furthermore, it provides both theoretical and practical foundations for the development of green, biodegradable, and high-performance starch-based thermoplastic materials. This approach holds considerable promise for applications in packaging, coatings, and functional composite materials.

COMPETING INTERESTS

The authors have no relevant financial or non-financial interests to disclose.

REFERENCES

- [1] X Luan, M Kumar, H Wang, et al. Dynamic material flow analysis of plastics in China from 1950 to 2050. *Resources, Conservation and Recycling*, 2021, 327: 129492.
- [2] M Kumar, S Sharma, Y Zhang, et al. Current research trends on micro- and nano-plastics as an emerging threat to global environment: A review. *Journal of Hazardous Materials*, 2021, 409: 124967.
- [3] W Ning, Y Zhao, C Liu, et al. The influence of citric acid on the properties of thermoplastic starch/linear low-density polyethylene blends. *Carbohydrate Polymers*, 2007, 67(3): 446–453.
- [4] B-T Wang, Q Zhang, Y Wang, et al. Studies of cellulose and starch utilization and the regulatory mechanisms of related enzymes in fungi. *Journal of Fungi*, 2020, 12(3): 530.
- [5] M Xu, Y Liu, J Wang, et al. Fabrication high toughness poly(butylene adipate-co-terephthalate)/thermoplastic starch composites via melt compounding with ethylene-methyl acrylate-glycidyl methacrylate. *Composites Part B: Engineering*, 2023, 250: 126446.
- [6] LZ Li, F Zhang, X Chen, et al. The effect of starch concentration on the gelatinization and liquefaction of corn starch. *Starch/Stärke*, 2015.
- [7] S Wang, J Liu, M Zhao, et al. Treatment and mechanism for hot melting starch by reducing the molecular chain winding and crystallinity. *International Journal of Biological Macromolecules*, 2024, 325: 121574.
- [8] H Xiao, Q Lin, G-Q Liu. Effect of cross-linking and enzymatic hydrolysis composite modification on the properties of rice starches. *Molecules*, 2012, 17(7): 8136–8146.
- [9] A Karim, Y Nadiha, O Nazuni, et al. Dual modification of starch via partial enzymatic hydrolysis in the granular state and subsequent hydroxypropylation. *Carbohydrate Polymers*, 2008, 56(22): 10901–10907.
- [10] B Kaur, D Ariffin, A Bhat, et al. Progress in starch modification in the last decade. *Food Hydrocolloids*, 2012, 26(2): 398–404.
- [11] A Gilet, T Martin, C Lefèvre, et al. Synthesis of 2-hydroxydodecyl starch ethers: Importance of the purification process. *Carbohydrate Polymers*, 2018, 58(7): 2437–2444.
- [12] W S Ratnayake, D S Jackson, et al. Phase transition of cross-linked and hydroxypropylated corn (*Zea mays* L.) starches. *LWT - Food Science and Technology*, 2008, 41(2): 346–358.
- [13] H Kong, Z Li, J Zhang, et al. Fine structure impacts highly concentrated starch liquefaction process and product performance. *Food Chemistry*, 2021, 164: 113347.
- [14] J Compart, A Schmidt, H Gruber, et al. Customizing starch properties: A review of starch modifications and their applications. *Polymers*, 2023, 15(16): 3491.
- [15] JN BeMiller. Effect of hydrocolloids on normal and waxy maize starches cross-linked with epichlorohydrin. *Food Hydrocolloids*, 2021, 112: 106260.
- [16] X Wang, L Chen, Y Li, et al. Crosslinking effect of dialdehyde starch (DAS) on decellularized porcine aortas for tissue engineering. *Acta Biomaterialia*, 2015, 79: 813–821.
- [17] B S Scopel, L B Silva, D S Andrade, et al. Starch-leather waste gelatin films cross-linked with glutaraldehyde. *Journal of Polymers and the Environment*, 2020, 28: 1974–1984.

- [18] R Lubczak, D Szczęch, et al. Polyurethane foams with starch. *Journal of Chemical Technology and Biotechnology*, 2019, 94(1): 109–119.
- [19] I Lipatova, A Yusova. Effect of mechanical activation on starch crosslinking with citric acid. *International Journal of Biological Macromolecules*, 2021, 185: 688–695.
- [20] Y Zhao, X Zheng, T Hu, et al. Cross-linked modification of tapioca starch by sodium trimetaphosphate: An influence on its structure. *Carbohydrate Polymers*, 2024, 23: 101670.
- [21] A S Babu, R Kumar, V Patel, et al. Chemical and structural properties of sweet potato starch treated with organic and inorganic acid. *Carbohydrate Polymers*, 2015, 52: 5745–5753.
- [22] P C Martins, L C Gutkoski, V G Martins. Impact of acid hydrolysis and esterification process in rice and potato starch properties. *International Journal of Biological Macromolecules*, 2018, 120: 959–965.
- [23] P Van Hung, T N Dung, T M Cuong, et al. Physicochemical characteristics and in vitro digestibility of potato and cassava starches under organic acid and heat-moisture treatments. *Food Chemistry*, 2017, 95: 299–305.
- [24] K Noulis, G Drosou, E Papadopoulou, et al. Sodium trimetaphosphate crosslinked starch films reinforced with montmorillonite. *Polymers*, 2023, 15(17): 3540.
- [25] H-S Kim, J H Lee, M S Park, et al. Cross-linking of corn starch with phosphorus oxychloride under ultra high pressure. *Carbohydrate Polymers*, 2012, 130(4): 977–980.
- [26] N Hu, F Zhang, J Li, et al. Synthesis and evaluation of microstructure of phosphorylated chestnut starch. *Starch/Stärke*, 2014, 37(1): 75–85.
- [27] Y Xie, Z Li, W Wang, et al. Effects of cross-linking with sodium trimetaphosphate on structural and adsorptive properties of porous wheat starches. *Food Chemistry*, 2019, 289: 187–194.
- [28] J Hu, X Wang, R Liu, et al. Dissolution of starch in urea/NaOH aqueous solutions. *Carbohydrate Polymers*, 2016, 133(19).
- [29] P Liu, H Zhang, M Fang, et al. Effects of different ratios of water and glycerol on the physicochemical properties of starch-based straws. *International Journal of Biological Macromolecules*, 2025, 466: 142215.
- [30] P Cheviron, F Gouanvé, E Espuche. Preparation, characterization and barrier properties of silver/montmorillonite/starch nanocomposite films. *Journal of Membrane Science*, 2016, 497: 162–171.